Jurnal Teknologi

RAPID INVESTIGATION OF THE METABOLITE CONTENT IN *HIBISCUS SABDARIFFA* var. UKMR-2 CULTIVATED UNDER THE INFLUENCE OF ELEVATED CO₂ USING TRI-STEP FT-IR SPECTROSCOPY

Siti Aishah Mohd Ali[a]*, Jalifah Latip[b]

[a]Faculty of Science and Natural Resources, Universiti Malaysia Sabah, Jalan UMS, 88400 Kota Kinabalu, Sabah, Malaysia
[b]Department of Chemical Sciences, Faculty of Science and Technology, Universiti Kebangsaan Malaysia, 43600 Bangi, Selangor, Malaysia

Graphical abstract

UKMR-2 | Dry calyx | Dry extract

IR spectrum

Heating jacket

SD-IR spectrum

Autopeak | Synchronous contour plot
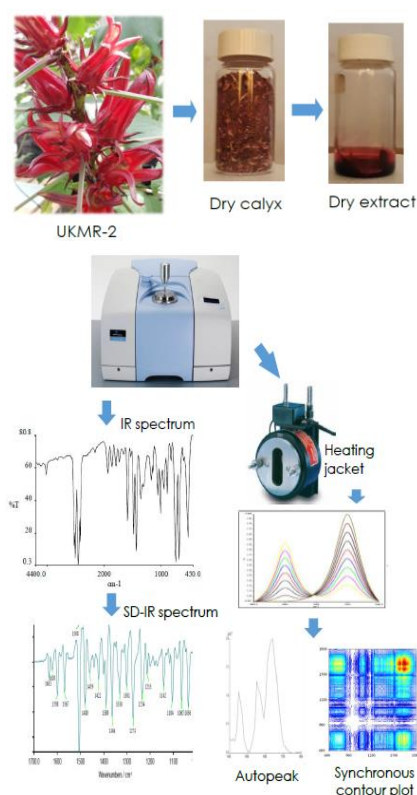
Abstract

Rapid methods based on untargeted analysis technique such as Fourier Transform Infrared (FT-IR) spectroscopy can provide much faster and easier solution for food authentication. However, studies on the metabolite content in UKMR-2 calyces using FT-IR spectroscopy has not been reported yet in any previous studies. Thus, the present study was performed to analyze the differences in metabolite content in UKMR-2 calyces under the influences of different [CO₂] treatment by applying tri-step infrared based fingerprinting. The UKMR-2 plant cultivation was exposed to ambient [CO₂] (400 µmol/mol) and elevated [CO₂] (800 µmol/mol) treatment. The UKMR-2 calyx extracts were analysed by conventional infrared (1D-IR), second derivative infrared (SD-IR) and two-dimensional correlation infrared (2D-IR) spectroscopy. The 1D-IR spectrum results revealed a similar absorption spectrum in the range of 1900 - 650 cm⁻¹, which suggest similar major metabolites content present in both extracts. For SD-IR spectrum, both treatments clearly showed have more peaks with different shape, position and intensity in the range of 1650 - 1450 cm⁻¹ and 1200 - 950 cm⁻¹, which is likely to have different flavonoid and carbohydrate content in UKMR-2 calyces. The 2D-IR synchronous correlation spectrum in the range of 1000 – 650 cm⁻¹ clearly distinguished the metabolite content in the UKMR-2 calyx extract from different [CO₂] treatment. Therefore, this tri-step infrared based fingerprinting has the potential as one of the effective methods to discriminate extract samples with similar infrared fingerprint features and indicate that the metabolite content in UKMR-2 calyces were influenced by different [CO₂] treatments.

Keywords: H. sabdariffa var. UKMR-2, elevated [CO₂], infrared based fingerprinting, second derivative infrared, 2D-IR synchronous correlation

Abstrak

Kaedah pantas berdasarkan teknik analisis tidak bersasar seperti spektroskopi inframerah transformasi Fourier (FT-IR) dapat melakukan pengesahan bahan makanan dengan yang lebih cepat dan mudah. Walau bagaimanapun, kajian mengenai kandungan metabolit dalam kaliks UKMR-2 menggunakan spektroskopi FT-IR masih belum pernah dilaporkan sebelum ini. Oleh itu, kajian ini dilakukan bagi melihat perbezaan kandungan metabolit dalam kaliks UKMR-2 yang ditanam di bawah pengaruh rawatan [CO₂] yang berbeza dengan

menggunapakai kaedah pencapjarian berasaskan inframerah tiga langkah. Penanaman pokok UKMR-2 dilakukan secara pendedahan kepada rawatan ambien [CO$_2$] (400 µmol/mol) dan peningkatan [CO$_2$] (800 µmol/mol). Ekstrak kaliks UKMR-2 dianalisis menggunakan spektroskopi inframerah konvensional (1D-IR), inframerah derivatif kedua (SD-IR) dan inframerah korelasi dua-dimensi (2D-IR). Hasil spektrum ID-IR mendedahkan spektrum penyerapan yang hampir sama dalam julat 1900 - 650 cm^{-1}, mencadangkan kedua-dua ekstrak mempunyai kandungan metabolit utama yang serupa. Bagi spektrum SD-IR, kedua-dua rawatan jelas menunjukkan kehadiran puncak yang lebih banyak dengan bentuk, kedudukan dan intensiti yang berlainan pada julat 1650 - 1450 cm^{-1} dan 1200 - 950 cm^{-1}, yang kemungkinan mengandungi sebatian flavonoid dan karbohidrat yang berbeza dalam kaliks UKMR-2. Spektrum korelasi *synchronous* 2D-IR pada julat 1000 - 650 cm^{-1} jelas membezakan kandungan metabolit dalam ekstrak kaliks UKMR-2 daripada rawatan [CO$_2$] yang berbeza. Oleh itu, pencapjarian inframerah berasaskan tiga langkah ini berpotensi sebagai salah satu kaedah yang berkesan dalam membezakan ekstrak sampel dengan ciri pencapjarian inframerah yang hampir serupa serta menunjukkan bahawa kandungan metabolit dalam kaliks UKMR-2 dipengaruhi oleh rawatan [CO$_2$] yang berbeza.

Kata kunci: *H. sabdariffa* var. UKMR-2, peningkatan [CO$_2$], pencapjarian berasaskan inframerah, inframerah derivatif kedua, korelasi *synchronous* 2D-IR

1.0 INTRODUCTION

The rapid development of the quality and nutritional properties in the food industry, especially in authenticity evaluation, characterizing metabolite content are usually determined by common techniques such as nuclear magnetic resonance (NMR), high-performance liquid chromatography (HPLC) and gas chromatography–mass spectroscopy (GC–MS). Most of these fingerprinting methods is expensive, time-consuming, high maintenance and mostly targeted to specific compounds. Thus, rapid screening analytical method such as mid-infrared (MIR) spectroscopy could be a suitable technique in this point to ensure the food quality and safety.

For a complex system, Fourier transform infrared (FT-IR) spectroscopy has shown advantages over the other spectroscopic analysis technique. FT-IR spectroscopy is one of the most available and flexible methods used for the untargeted analysis approach, being simple, fast and non-destructive, robust, high specificity and easy preparation with small amount of samples [1]. FT-IR spectroscopy is a physico-chemical method that measures the vibrations mode of each functional group for the whole features in the sample. It generates an absorption peak in the infrared spectrum that can be regarded as metabolic fingerprint characters [2]. Owing to the fingerprint features and extensively applied to the natural product samples, FT-IR has played an essential role in research on various aspects, especially in food analysis and non-destructive applications [2-4]. For instance, recent studies showed FT-IR were used to differentiate extra virgin olive oils and Propolis from different geographical origins [4-6] and different genetic varieties [7]. The IR analysis also an excellent tool to

provide quantitative information of complex matrices since the intensities of the absorption peaks is proportional to concentration [8]. The addition of second derivative infrared (SD-IR) scanning enhance the overlapped peaks resolution, while the two-dimensional correlation infrared (2D-IR) improve spectrum resolution by a dynamic changes of thermal perturbation to obtain more chemical correlation information [9-10].

Hibiscus sabdariffa (roselle) also known as *asam paya* in Malaysia [11] has tremendous potential in many industries such as food colorant, health associated products and many others [12]. The red calyx has high amount of phenolic compounds (anthocyanins, phenolic acids), alkaloids, steroids, flavonoids, saponins, ascorbic acid as well as minerals [12-14]. Roselle that has many therapeutic potentials also used as an antioxidant, anti-diabetic, anti-hypertensive, anti-cancer agents and useful for cardio protective action [15-17]. *Hibiscus sabdariffa* var. UKMR-2 was produced by mutation breeding has several unique characteristics (shorter life cycle, higher yield of calyces per plant, higher lodging resistance) as compared to their parent variety 'Arab' and other varieties [18].

At present, extensive studies related to climate impacts on major food crops showed elevated CO$_2$ has significant influence on carbohydrate and carbon-based secondary metabolites production such as flavonoid, tannin, phenolic and ascorbic acid [19-21]. Photosynthesis rate can be stimulated by elevated CO$_2$ which leads to increased assimilation and carbon uptake, thereby increasing the secondary metabolites accumulation [21]. However, different food crops respond differently to elevated CO$_2$ exposure. Therefore, this study was performed to report the

holistic variation on the metabolite production in *H. sabdariffa* var. UKMR-2 extract by applying conventional infrared (1D-IR), second derivative infrared (SD-IR) and 2D-IR correlation to classify the inherent qualities of UKMR-2 calyces under the influences of different [CO_2] treatments.

2.0 METHODOLOGY

2.1 Plant Samples and Treatments

UKMR-2 plant cultivation and calyx extract preparation were performed using the method described by Siti Aishah *et al.* [22]. Briefly, two levels of [CO_2] treatment was started from August until December 2017 (after transplanting); ambient [CO_2] at approximately 400 µmol/mol as the control of greenhouse and elevated [CO_2] with approximately 800 µmol/mol in the open roof ventilation greenhouse system (ORVS) were exposed to UKMR-2. The elevated CO_2 treatment was done by daily automated continuous injection of pure CO_2 for 2 hours in the chamber and monitored using CO_2 analyzer. The elevated CO_2 with 800 µmol/mol value intended to represent the predicted range of atmospheric CO_2 concentration at the end of the 21st century from a global climate model under WGIII scenario [23]. UKMR-2 calyces were harvested within 28-30 day after flowering started at the end of November until December 2017 from six individual plants per treatments as biological replicates. The fresh calyces were air dried at room temperature, extracted with water in a ratio of 1:10 and dried using Alpha 1-2 LDplus freeze dryer (Martin Christ, Germany) to produce water crude extract.

2.2 Apparatus

Infrared (IR) analyses were performed on the Perkin Elmer Spectrum 400 FT-IR/FT-NIR Spectroscopy. The data were processed using Perkin Elmer Spectrum version 10.5.3 software (USA). For 2D FT-IR, Specac Heated Jacket Controller (Kent, UK) was used to perform the thermal perturbation. The 2D spectrum was analyzed with TD version 0.54 software developed by the Analysis Center of the Chemistry Department, Tsinghua University.

2.3 1D and 2D FT-IR Procedures

About 1 mg of UKMR-2 freeze-dried extracts were mixed with 200 mg dehydrated potassium bromide (KBr) powder. The sample mixture was further processed until a thin pellet was formed. The KBr pellet was positioned on the FT-IR spectroscopy sample reservoir for the spectrum capture. Six biological with three technical replicates UKMR-2 crude extract from each treatment were recorded to generate a representative 1D-IR spectrum after a total of 32 scans at a range of 4000 - 650 cm^{-1} to 4 cm^{-1} resolution. The second derivative IR spectrum was obtained after

Savitzky-Golay polynomial fitting with intermediate 13-points smoothing at room temperature. For 2D FT-IR, the temperature range is from 40 to 120 °C and spectrum were collected every 10 °C. The dynamic spectrum was analyzed and transformed into 2D synchronous contour plot and auto-peak spectrum.

3.0 RESULTS AND DISCUSSION

3.1 Conventional Infrared (1D-IR) Spectrum Analysis of UKMR-2 Calyx Extracts

Before starting the IR spectrum analysis, only the 'fingerprint region' between 1900 and 650 cm^{-1} for all spectrums were cut and selected for analysis. This fingerprint region is rich with structural information, showing many bands specific to molecular structure and mostly overlapping each other. Generally, the spectrum region between 4000 - 2500 cm^{-1} in UKMR-2 calyx extract for both [CO_2] treatments mainly have a broad band, which associated with hydroxyl (-OH) and aromatic C-H stretching vibrations [24]. Meanwhile, the range between 2500 - 1900 cm^{-1} did not contain relevant information. Therefore, the fingerprint region between 1900 - 650 cm^{-1} was selected in detail in order to characterize metabolites compound families in the UKMR-2 extract.

Figure 1 represent the comparative fingerprint zone (1900 - 650 cm^{-1}) 1D-IR spectrum of UKMR-2 extracts from elevated (e[CO_2]) and ambient (a[CO_2]) treatments, while Table 1 showed the holistic assignment of each peak in the IR spectrum. Considering UKMR-2 calyx extract is a complex mixture, its 1D-IR spectrum contains several overlapping absorption peaks from different functional groups. As expected, the 1D-IR spectrum for both [CO_2] treatment shows a similar absorption spectrum of various components, differing only in the intensity, which suggest similar major metabolite contents present in both extracts. In the infrared fingerprint region, several absorption peaks features can be extracted such as the peak at 1607 cm^{-1} was assigned to the C=C bonds stretching vibration in aromatic rings compounds, and the peaks at 1221 – 1030 cm^{-1} were attributed to C–O stretching vibration, which displayed the fingerprint features of glycosides. In addition, the strong peak at 1800 and 1700 cm^{-1} in both fingerprint area are corresponded to the stretching vibrations of C=O group, normally refers to ester components or acid anhydride group [25]. These data indicate that the major content in UKMR-2 calyces have their own infrared characteristic peaks.

Previous studies showed that roselle calyces rich with anthocyanins, phenolic acids and flavonoids [12-14, 22]. Plant phenolics are a chemically heterogeneous groups, consist at least one hydroxyl functional group on an aromatic ring(s) [26]. The phenolic compound IR spectrum showed common absorption peaks associated with aromatic six-membered rings and hydroxyl moieties. According to

Abbas *et al.* [27], the phenolic acids were characterized in infrared spectrum mainly by absorption peaks of alkenes, unsaturated carboxylic acids and esters vibration mode, whereas flavonoids compound were characterized mainly by absorption peaks associated with benzopyrylium, benzo-γ-pyrone and 2-phenyl-3,4-dihydro-2H-chromen-3-ol vibration mode.
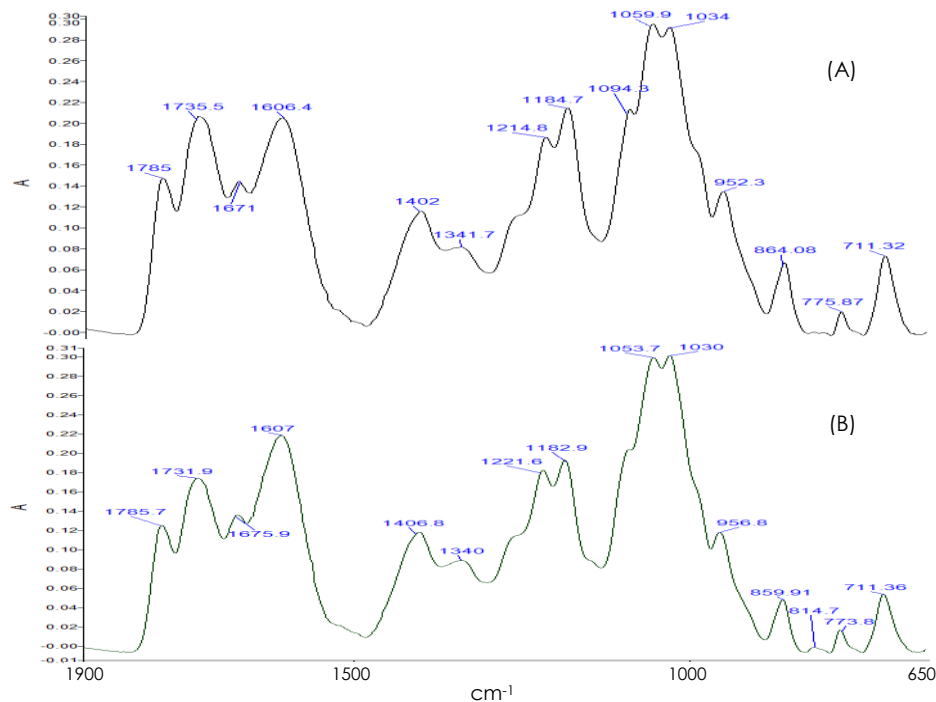

Figure 1 1D-IR spectrum of the UKMR-2 calyx extracts in the range of 1900 – 650 cm^{-1}; (A) a[CO_2] and (B) e[CO_2]

Table 1 Infrared spectral assignment of *H. sabdariffa* var. UKMR-2 extracts [24, 25-26, 30-31]

Band (cm⁻¹)	Vibration mode	Main attribution	CO_2 Treatment	
			Ambient	Elevated
1775 - 1740	v C=O	Anhydrides	1785	1785
1750 - 1735	v C=O	Ester, aldehyde, saturated aliphatic, Carbocylic acid	1735	1731
1670-1630	v C=C (isolated), v -C=C-	Alkenes	1671	1675
1640 - 1610	v C=C (conjugated)	Alkenes	1606	1607
1440 - 1400	δ O-H, v_{as} (COO⁻)	Carbocylic acid, ester, or carbonyl groups	1402	1406
1350-1310	δ C-OH, v C-O, δ C-H in-plane	Carbocylic acid, Alkenes	1341	1340
1250 - 1120	v C-O, v C-O-C (dialkyl)	Alcohol, Carbocylic acid, ethers	1214	1221
1210 - 1160	v C-C(O)-C	Ester, Anhydrides	1184	1182
1260 - 1000	v C-O, v C-O-C (dialkyl)	Alcohols, ethers	1094	-
1260 - 1000	v C-O	Alcohols	1059	1053
1260 - 1000	v C-O	Alcohols	1034	1030
950 - 910	δ O-H out-of-plane	Carbocylic acid	952	956
850 - 800	δ C-H (para)	Aromatics	864	859
815	δ C-H (trisubstituted)	Alkenes	-	814
770 - 730	δ C-H (ortho)	Aromatics	775	773
720	δ C-H, O-H out-of-plane	Alkanes, Aromatics (mono)	711	711

Note: v, stretching vibration; δ, bending; as, asymmetrical vibration

A phenolic acids could be distinguished by absorption peaks between 1755 - 1630 cm^{-1} for carboxylic acid vibration, while for flavonoids were characterized by numerous absorption peaks in the range of 1650 – 1400 cm^{-1} and 1200 cm^{-1} [27]. Chlorogenic acid were characterized mainly by the presence of α,β-unsaturated aliphatic ester or the carbonyl (C=O) stretching vibration around 1720 cm^{-1}

[28-29]. Further, the peaks between 1200 - 950 cm^{-1} indicated content of carbohydrate in roselle extracts. Therefore the content of carbohydrate in both extracts was almost the same level. Lu *et al.* [30] stated that the bands between 1170 - 930 cm^{-1} can be predominantly assigned to polysaccharides or flavonoids, with high intensity bands by the presence of flavonol glycosides, compounds which have alcohol as primary functional group. The 900 – 700 cm^{-1} spectral region is associated with C-H bending from the aromatic compounds from out-of-plane deformation vibrations [31]. Abbas *et al.* [27] states that this region is important to determine the type of aromatic substitution in phenolic compound. In addition, broad absorption peaks appear around 720 cm^{-1} associated to the out-of-plane deformation of the hydroxyl group [32]. Some shifts existence in the absorption peaks in the infrared spectrum is due to the presence of several hydroxyl groups in different positions and due to glucoside molecules in phenolic compounds [27].

The fingerprint zone 1D-IR spectrum is divided into three areas (1800 - 1500, 1499 - 900 and 899 - 650 cm^{-1}) and represented most of the primary and secondary metabolites. Despite the shared common fingerprint features, one can observe the different intensities, shapes and positions of the prominent peaks between different [CO_2] treatments. Comparison of the 1D-IR spectrum of a[CO_2] (Figure 1A) and e[CO_2] extract (Figure 1B) revealed that these two extracts have first four peaks in the first region from the range of 1800-1600 cm^{-1}. However, two of the first peaks at 1785 and 1735 cm^{-1} in a[CO_2] extract have higher intensity as compared to e[CO_2]. Meanwhile, the two peaks of a[CO_2] spectrum at 1731 and 1606 cm^{-1} were almost at the same level of intensity, while in e[CO_2] spectrum showed peak at 1731 cm^{-1} were lower than 1607 cm^{-1}. Different intensities in the range of 1800 – 1600 cm^{-1} indicate the possibility of differences in phenolic acid content influenced by [CO_2] treatment.

A bit dissimilarity of the absorption peaks in the range of 1150 - 800 cm^{-1} in term of their position, shape and intensity, while some peak was absent in other spectrum. Both extracts showed twin peaks with the highest absorbance at the range of 1100 – 1000 cm^{-1}. However, the twin peak of e[CO_2] spectrum at 1053 and 1030 cm^{-1} were almost at the same level, while in a[CO_2] spectrum showed peak at 1034 cm^{-1} were lower than 1059 cm^{-1}. The twin peak is characteristic of the C - O stretch vibration, which refer as glucose with the highest absorption peak at 1033 cm^{-1}, while for fructose has specific marker absorption peak at 1063 cm^{-1} [33]. Meanwhile, a small peak at 814 cm^{-1} detected only in e[CO_2] spectrum, while a small shoulder peak 1093 cm^{-1} was detected in a[CO_2] spectrum. Furthermore, the peaks at 1184, 952, 864 and 711 cm^{-1} have higher intensity in a[CO_2] spectrum rather than e[CO_2] spectrum.

The present study of 1D-IR spectrum UKMR-2 calyx spectrum was also compared with *H. sabdariffa* L. extract from Choong *et al.* [25] and anthocyanin standard. Both roselle varieties have a similar pattern of peaks from the range of 1800 - 1600 cm^{-1}. The main differences between the two varieties can be seen in the range of 1350 – 950 cm^{-1}, five peaks can be seen and reported in *H. sabdariffa* L. extract and seven sharp peaks in UKMR-2 extract. This suggests that there may be differences in metabolite compounds between the two roselle varieties. The comparison with delphinidin-3-*O*-sambubioside and cyanidin-3-*O*-sambubioside standard were categorized into three sections: 1900-1550 cm^{-1}, 1549-1000 cm^{-1} and 999-650 cm^{-1}. The absence of any peak at the beginning section of 1900-1700 cm^{-1} was observed in both anthocyanin standards. For these standards, the main absorbance peaks were located in the range of 1650-800 cm^{-1}, which was also found in the second and third sections of the UKMR-2 extracts. The peak 1059/1053 cm^{-1} in UKMR-2 extract was comparable in both anthocyanin standards. In addition, another five peaks around 1214/1221, 1184/1182, 1034/1030, 864/859 and 711 cm^{-1} in UKMR-2 extracts were also associated well with delphinidin-3-*O*-sambubioside. Meanwhile, another four peaks around 1341/1340, 1214/1221, 1184/1182 and 814 cm^{-1} matched with cyanidin-3-*O*-sambubioside. Therefore, UKMR-2 extracts showed the existence of anthocyanin content.

3.2 Second Derivation (SD-IR) Spectrum Analysis of UKMR-2 Calyx Extracts

Figure 2 shows the second derivative (SD-IR) spectrum of UKMR-2 extract in the region of 1900 – 650 cm^{-1}, which contains the main absorption peaks of the metabolite content in the extracts. The SD-IR spectrums were used to enhance the apparent resolution of the 1D-IR spectrums and to amplify small differences in the infrared spectrum [31].

There were more obvious peaks were detected in SD-IR spectrum albeit of different relative intensities. Both calyx extracts have a congested region of base peaks in the range of 1650 - 1450 cm^{-1}. The congested region for a[CO_2] has more small peaks compare to e[CO_2] extract, which is likely to have different flavonoid content [27]. Moreover, eight peaks were occurring in the spectral region between 1200 - 950 cm^{-1} (mainly from carbohydrates) for both extracts with a bit different in term of their position, shape and intensity [30]. According to Agatonovic-Kustrin *et al.* [35], the cyclic nature of the ether group (aromatic C-O bond stretching) was reflected by the peaks located in the range of 1272 - 1266 cm^{-1} and 1186 - 1177 cm^{-1}.

A distinctive sharp absorption peak, which occurred at 909 cm^{-1} in a[CO_2] extract and 814 cm^{-1} in e[CO_2] extract can be a characteristic feature to distinguish between both UKMR-2 extracts. For e[CO_2] extract, the intensity of the peak at 1148 cm^{-1} is higher as compared to a[CO_2] extract at 1141 cm^{-1}. Moreover, two small peaks in e[CO_2] the range between 1053 - 1030 cm^{-1} of 1D-IR has been derived into three peaks in SD-IR spectrum. The peaks in this range mainly attributed to the C–O stretching

vibration, the characteristic of primary alcohol functional group absorptions [24]. In contrast, a very small peak at 1094 cm^{-1} of a[CO_2] 1D-IR produce a very sharp two peaks in SD-IR spectrum. Therefore,

these two UKMR-2 extracts can be distinguish by fingerprint characters by the enhance resolution in the SD-IR spectrum.
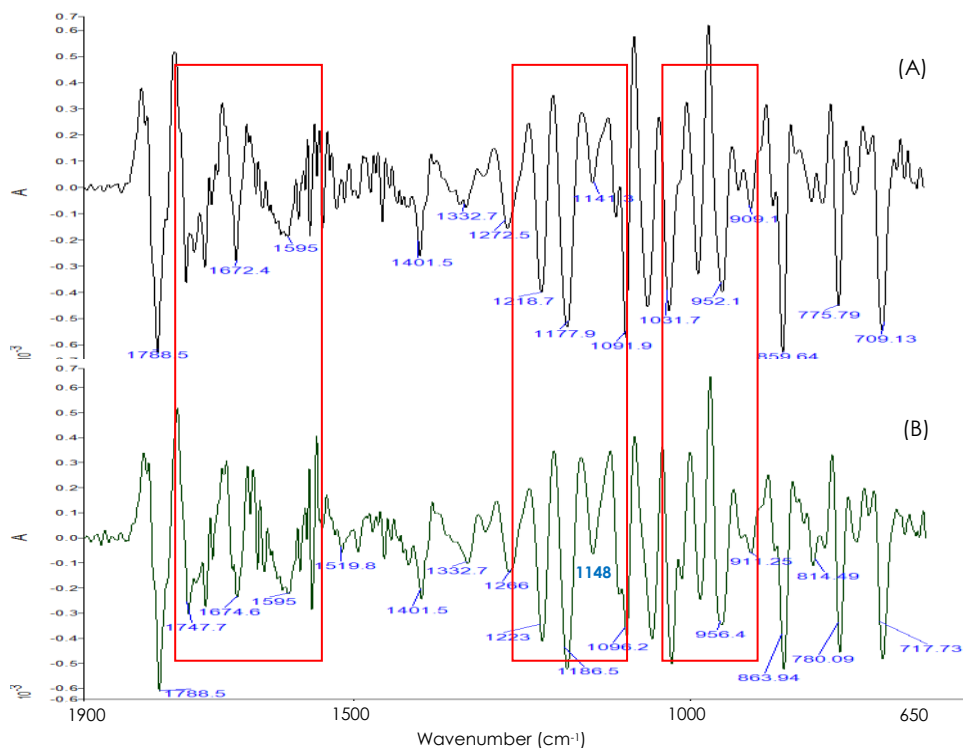

Figure 2 SD-IR spectrum of the UKMR-2 calyx extracts in the range of 1900 – 650 cm^{-1}; (A) a[CO_2] and (B) e[CO_2]. The main differences of both spectrums were highlighted in box

3.3 Two-Dimentional Correlation IR (2D-IR) Spectrum Analysis of UKMR-2 Calyx Extracts

Two-dimensional infrared (2D-IR) synchronous correlation spectrum was applied to identify differences among the complex samples in a more convincing and visual way. Wang *et al*. [36] stated that 2D-IR correlation spectrum can enhance the resolution of the 1D-IR spectrums to a given thermal perturbation and acquire the information of sub molecular interaction between functional groups. In order to improve the spectral resolution, 2D-IR synchronous correlation spectrum was formed based on thermal disturbances sample in the range of 40 to 120 °C. According to Xu *et al*. [37], the auto-peaks on the diagonal line in the 2D-IR synchronous spectrum show the self-correlativity and susceptibility of certain absorption band. These auto-peaks produced the variation of spectral intensity through thermal treatment. Meanwhile, the cross-peaks locating at the off-diagonal position indicate the vibrational correlativity between two different functional groups [37]. The closer the correlativity is, the stronger the intensity of cross-peak will be [10]. The positive correlation (red or yellowish area) in synchronous correlation spectrum means that a group of absorption bands change simultaneously either

become stronger or weaker signal, while negative correlation (blue area) is just the reverse situation [37].

Figure 3 (A1 and B1) showed a noticeable similarity in the synchronous 2D-IR contour plot of the two [CO_2] treatments in the range between 1800 – 1000 cm^{-1}, mainly exhibit the characteristic absorption of carbonyls and olefinic bonds. This spectrum indicates the holistic view of perturbed reaction of the different types of compound in the UKMR-2 extract. In order to see the cross-peak correlation, both spectrum exhibit three correlation squares formed with negative cross-peaks. The first correlation square created at 1619 cm^{-1} with 1168 cm^{-1} correlated with negative cross-peaks at (1168, 1619) and (1619, 1168). Another bigger correlation square which is created by cross-peaks at 1761 cm^{-1} and 1619 cm^{-1}, correlated negatively at (1619, 1761) and (1761, 1619). The third correlation with smaller square is created by 1379 cm^{-1} and 1619 cm^{-1} with negative cross-peaks at (1619, 1379) and (1379, 1619). However, the third positive correlation showed weaker signal in a[CO_2] spectrum than e[CO_2]. Both spectrums also showed positive cross-peaks with an interval of 50 cm^{-1} (yellowish colour in the upper right corner) in the range 1750 - 1550 cm^{-1}. There were also two small correlation squares with weak positive cross-peaks recorded at (1168, 1761) and (1379, 1168) cm^{-1}. According to Choong [38], 2D-IR spectrum of *H.*

sabdariffa L. extract with trifluoroacetic acid (TFA) formed three correlation squares; negative cross-peaks (720, 1771), negative cross-peaks (720, 1168), and positive cross-peaks (1168, 1771) which are correlated with the C-O bond from the ester group with carbohydrate group.
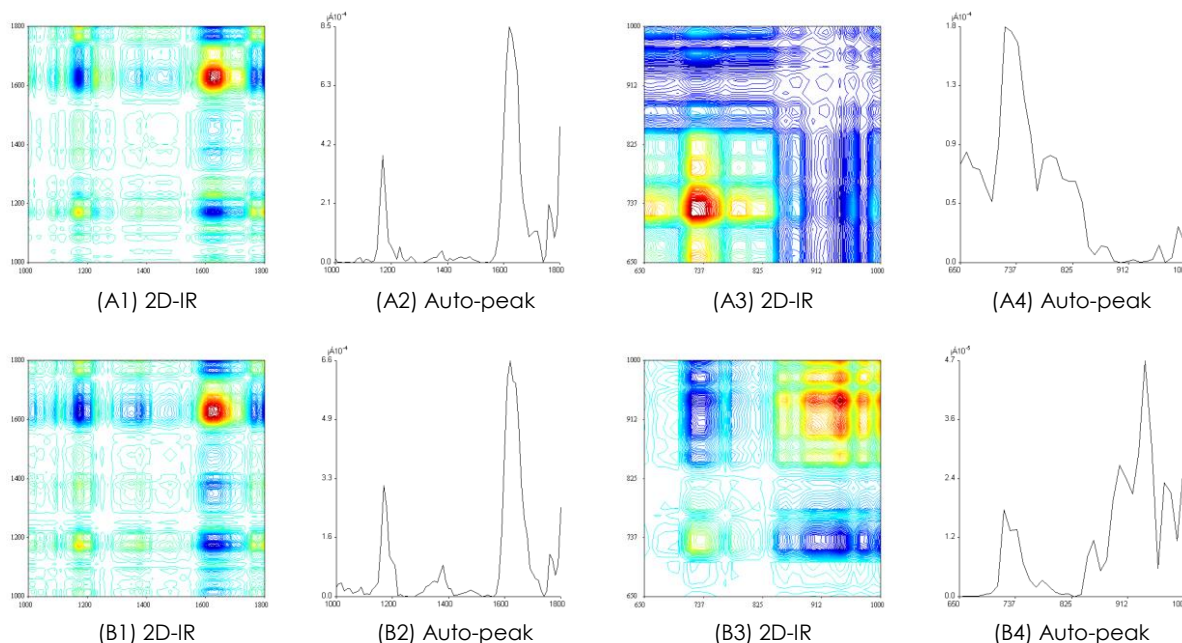

Figure 3 2D-IR synchronous and auto-peak spectrum of the UKMR-2 calyx extracts; (A1) a[CO_2] 2D-IR in the range 1800-1000 cm^{-1}, (A2) a[CO_2] auto-peak in the range 1800-1000 cm^{-1}, (A3) a[CO_2] 2D-IR in the range 1000-650 cm^{-1}, (A4) a[CO_2] auto-peak in the range 1000-650 cm^{-1}, (B1) e[CO_2] 2D-IR in the range 1800-1000 cm^{-1}, (B2) e[CO_2] auto-peak in the range 1800-1000 cm^{-1}, (B3) e[CO_2] 2D-IR in the range 1000-650 cm^{-1}, (B4) e[CO_2] auto-peak in the range 1000-650 cm^{-1}

From the auto-peak spectrum in the range 1800 -1000 cm^{-1} (Figure 3 A2 and B2), the result showed that the overall relative intensity in a[CO_2] spectrum is stronger than the e[CO_2]. Moreover, both [CO_2] treatments showed similar one strong major auto-peak at 1619 cm^{-1} and one weak auto-peak at 1168 cm^{-1}. In addition, the spectrum of e[CO_2] shows a bit higher intense auto-peak at 1377 cm^{-1} compare to a[CO_2] spectrum. The 1377 cm^{-1} absorption peak attributes to the O-H in plane deformation in polyphenols [36]. Similarly, small weak peaks at 1229 and 1269 cm^{-1} are only visible in a[CO_2].

Another intense range of 1000 – 650 cm^{-1} synchronous 2D-IR contour plot is presented in Figure 3 (A3 and B3). The overall relative intensity in a[CO_2] spectrum was higher than e[CO_2]. The contour or stereo-fish-net patterns were also different between both treatments, indicate that the dissimilar metabolite content of the UKMR-2 extract. There is a very clear illustration of correlation squares with positive cross-peak at the range from 850 - 650 cm^{-1} (yellowish colour with an interval of 50 cm^{-1}) for a[CO_2] spectrum, meanwhile the correlation squares

with positive cross-peak for e[CO_2] were found at the upper right corner from 1000 – 850 cm^{-1}. By contrast, four strong correlations square with negative cross-peaks were recorded only in e[CO_2] at (720, 860), (720, 900), (720, 938) and (720, 970) cm^{-1}.

From the auto-peak spectrum (Figure 3 A4 and B4), one strong auto-peak was apparent in a[CO_2] and e[CO_2] treatment near 720 and 938 cm^{-1}, respectively with differing in their relative intensities. Both auto-peak were surrounded by two correlation squares with positive cross-peaks in a[CO_2] and e[CO_2] spectrum, indicating that the centralized peak was important and correlated with many compounds crossing with it. Peaks around 920 - 705 cm^{-1} are attributed to additional vibrations associated with C-H out-of-plane vibrations from anthocyanin bands based on the tetra-substituted pyrylium nucleus [40], while range between 1200 - 900 cm^{-1} contains functional groups for carbohydrates (sucrose, glucose and fructose) [30, 41]. For easy comparison, the information on the positions and correlations of the auto-peaks in Figure 3 are summarized in Table 2.

Table 2 The auto-peaks from 2D-IR correlation spectrum of the UKMR-2 calyx extracts from different $[CO_2]$ treatments

CO_2 Treatment	Auto-peak (cm^{-1})											
a$[CO_2]$	658	678	721	790	830	959	990	**1168**	1229	1318	**1619**	1715	1763
e$[CO_2]$	720	738	780	860	900	938	970	**1168**	1377	**1619**	1763

Notes: Peak values in bold show relative intensity > 40% (strong auto-peak), while peak values in underline are in negative correlation with other auto-peak

The 2D-IR correlation spectrum of both treatments has their own fingerprints characteristic which can be used as the exclusive range for discrimination. The overall 2D-IR synchronous correlation spectrum clearly distinguished the metabolite contents in UKMR-2 calyces from $[CO_2]$ treatments, due to differences in carbohydrate, phenolic acids, flavonoids and anthocyanins content. Further studies by using FT-IR metabolomic - chemometric approaches should be conducted to clearly identify which metabolites content in UKMR-2 calyces contributes to the discrimination between $[CO_2]$ treatments.

4.0 CONCLUSION

By using tri-step infrared based fingerprinting (1D-IR, SD-IR and 2D-IR correlation), the differences in metabolite production in UKMR-2 calyces under the influences of different $[CO_2]$ treatments can be determined. The overlapped peaks in the fingerprint region were identified and compared based on fingerprint characters, shapes, positions and intensities of the absorption peaks. In general, the UKMR-2 calyx extract for both $[CO_2]$ treatments can be clearly distinguished from each other through 2D-IR correlation spectrum in the range of 1000 – 650 cm^{-1}. These indicate that the metabolite content in UKMR-2 calyces was affected by different $[CO_2]$ treatments and proved that the tri-step infrared based fingerprinting is one of the effective methods to distinct differences between samples with similar infrared fingerprint characters.

Acknowledgement

References

[1]   Bureau, S., Ruiz, D., Reich, M., Gouble, B., Bertrand, D., Audergon, J., and Renard, C. 2009. Application of ATR-FTIR for a Rapid and Simultaneous Determination of Sugars and Organic Acids in Apricot Fruit. *Food Chemistry.* 115(3): 1133-1140.
      DOI: https://doi.org/10.1016/j.foodchem.2008.12.100.
[2]   Zuo, L., Sun, S.Q., Zhou, Q., Tao, J. X., and Noda, I. 2003. 2D-IR Correlation Analysis of Deteriorative Process of Traditional Chinese Medicine 'Qing Kai Ling' Injection. *Journal of Pharmaceutical and Biomedical Analysis.* 30(5): 1491-1498.
      DOI:http://dx.doi.org/10.1016/s0731-7085(02)00485-5.
[3]   Xu, C. H., Sun, S. Q., Guo, C. Q., Zhou, Q., Tao, J. X., and Noda, I. 2006. Multi-steps Infrared Macro-fingerprint Analysis for Thermal Processing of *Fructus viticis*. *Vibrational Spectroscopy* 41(1): 118-125.
      DOI: https://doi.org/10.1016/j.vibspec.2006.01.014.
[4]   Wu, Y. W., Sun, S. Q., Zhao, J., Yi, L., and Zhou, Q. 2008. Rapid Discrimination of Extracts of Chinese Propolis and Poplar Buds by FT-IR and 2D-IR Correlation Spectroscopy. *Journal of Molecular Structure.* 833-884: 48-50.
      DOI: https://doi.org/10.1016/j.molstruc.2007.12.009.
[5]   Selaimia, R., Oumeddour, R., and Nigri, S. 2017. The Chemometrics Approach Applied to FTIR Spectral Data for the Oxidation Study of Algerian Extra Virgin Olive Oil. *International Food Research Journal.* 24(3): 1301-1307.
[6]   Schulz, H., and Baranska, M. 2007. Identification and Quantification of Valuable Plant Substances by IR and Raman Spectroscopy. *Vibrational Spectroscopy.* 43(1): 13-18.
      DOI: https://doi.org/10.1016/j.vibspec.2006.06.001.
[7]   Salbiah Man., Ling Sui Kiong., Nor Azlianie Ab'lah., and Zunoliza Abdullah. 2015. Differentiation of the White and Purple Flower forms of *Orthosiphon aristatus* (Blume) Miq. By 1D and 2D Correlation IR Spectroscopy. *Jurnal Teknologi (Sciences & Engineering).* 77(3): 81-86.
[8]   Ferreira, D., Barros, A., Coimbra, M. A., and Delgadillo, I. 2001. Use of FTIR Spectroscopy to Follow the Effect of Processing in Cell Wall Polysaccharide Extracts of a Sun-dried Pear. *Carbohydrate Polymers.* 45(2): 175-182.
      DOI: https://doi.org/10.1016/S0144-8617(00)00320-9.
[9]   Noda, I. 1986. Two-dimensional Infrared (2D IR) Spectroscopy. *Bulletin of the American Physical Society.* 31: 520-524.
[10] Noda, I. 1989. Two-dimensional Infrared Spectroscopy. *Journal of the American Chemical Society.* 111(21): 8116-8118.
      DOI: https://doi.org/10.1021/ja00203a008.
[11] Wong, P. K., Salmah, Y., Ghazali, H. M., and Che Man. Y. B. 2002. Physico- Chemical Characteristics of Roselle (*Hibiscus sabdariffa* L.). *Nutrition and Food Science.* 32(2): 68-73.
[12] Puro, K., Sunjukta, R., Samir, S., Ghatak, S., Shakuntala, I., and Sen, A. 2014. Medicinal Uses of Roselle Plant (*Hibiscus sabdariffa* L.): A Mini Review. *Indian Journal of Hill Farming.* 27(1): 81-90.
[13] Obouayeba, A. P., Djyh, N. B., Diabate, S., Djaman, A. J., N'guessan, J. D., Kone, M., and Kouakou, T. H. 2014. Phytochemical and Antioxidant Activity of Roselle (*Hibiscus sabdariffa* L.) Petal Extracts. *Research Journal of Pharmaceutical, Biological and Chemical Sciences.* 5(2): 1453-1465.
[14] Ajoku, G. A., Okwute, S.K., and Okogun, J. I. 2015. Isolation of Hexadecanoic Acid Methyl Ester and 1,1,2-ethanetricarboxylic acid- 1-hydroxy-1, 1-dimethyl ester from the Calyx of Green *Hibiscus sabdariffa* (Linn). *Natural Products Chemistry & Research.* 3(2): 1-5.
      DOI : http://dx.doi.org/10.4172/2329-6836.1000169.
[15] Idris, M. H. M., Siti Balkis, B., Mohamad, O., and Jamaludin, M. 2012. Protective Role of *Hibiscus sabdariffa* Calyx Extract Against Streptozotocin Induced Sperm Damage in Diabetic Rats. *EXCLI Journal.* 11: 659-669.

[16] Satirah, Z., Siti Nor Farhanah, S. N. S., and Siti Balkis, B. 2016. *Hibiscus sabdariffa* Linn. (Roselle) Protects Against Nicotine-Induced Heart Damage in Rats. *Sains Malaysiana*. 45(2): 207-214.

[17] Lislivia, Y., Siti Aishah, M. A., Jalifah, L., Norsyahida, M. F., Siti Balkis, B., and Satirah, Z. 2017. Roselle is Cardioprotective in Diet-Induced Obesity Rat Model with Myocardial Infarction. *Life Sciences*. 191: 157-165.
DOI : http://dx.doi.org/10.1016/j.lfs.2017.10.030.

[18] Osman, M., Golam, F., Saberi, S., Majid, N. A., Nagoor, N. H. and Zulqarnain. M. 2011. Morpho-agronomic Analysis of Three Roselle (*Hibiscus sabdariffa* L.) Mutants in Tropical Malaysia. *Australian Journal of Crop Science*. 5(10):1150-6.

[19] Weigel, H. J., and Manderscheid, R. 2016. FACE with Crops: Data for Climate Change Impact Models. Braunschweig: Johann Heinrich von Thünen-Institut, 6 p, Thünen à la carte 4a.
DOI: http://dx.doi.org/10.3220/CA1455111790000.

[20] De Souza, A. P., Cocuron, J., Garcia, A. C., Alonso, A. P., and Buckeridge, M. S. 2015. Changes in Whole-plant Metabolism During the Grain-filling Stage in Sorghum Grown under Elevated CO_2 and Drought. *Plant Physiology*. 169: 1755-1765.
DOI: http://dx.doi.org/10.1104/pp.15.01054.

[21] Goufo, P., Pereira, J., Figueiredo, N., Beatriz, M., Oliveira, P. P., Carranca, C., Rosa, E. A. S., and Trindade, H. 2014. Effect of Elevated Carbon Dioxide (CO_2) on Phenolic Acids, Flavonoids, Tocopherols, Tocotrienols, γ-Oryzanol and Antioxidant Capacities of Rice (*Oryza sativa* L.). *Journal of Cereal Science*. 59:15-24.
DOI : http://dx.doi.org/10.1016/j.jcs.2013.10.013.

[22] Siti Aishah, M. A., Che Radziah, C. M. Z., and Jalifah, L. 2019. Influence of Elevated CO_2 on the Growth and Phenolic Constituents Production in *Hibiscus sabdariffa* var. UKMR-2. *Jurnal Teknologi*. 81(3): 109-118.
DOI: https://doi.org/10.11113/jt.v81.13241.

[23] IPCC. 2014: *Climate Change 2014: Synthesis Report. Contribution of Working Groups I, II and III to the Fifth Assessment Report of the Intergovernmental Panel on Climate Change,* edited by Core Writing Team, Pachauri, R.K. and Meyer, L.A. IPCC, Geneva, Switzerland. 151.

[24] Pavia, D., Lampman, G., Kriz, G., and Vyvyan, J. 2014. *Introduction to Spectroscopy*. Stamford: Cengage Learning.

[25] Choong, Y. K., Yousof, N. S. A. M., Wasiman, M. I., Jamal, J. A., and Ismail, Z. 2016. Determination of Effects of Sample Processing on *Hibiscus sabdariffa* L. using Tri-step Infrared Spectroscopy. *Journal of Analytical & Bioanalytical Techniques*. 7(5): 1-9.
DOI: http://dx.doi.org/10.4172/2155-9872.1000335.

[26] Taiz, L., and Zeiger, E. 2010. *Plant Physiology*. Sunderland: Sinauer Associates.

[27] Abbas, O., Compère, G., Larondelle, Y., Pompeu, D., Rogez, H., and Baeten, V. 2017. Phenolic Compound Explorer: A Mid-infrared Spectroscopy Database. *Vibrational Spectroscopy*. 92: 111-118.
DOI: http://dx.doi.org/10.1016/j.vibspec.2017.05.008

[28] Socrates, G. 1997. *Infrared Characteristic Group Frequencies*. Chichester: J. Wiley & Sons.

[29] He, J., Rodriguez-Saona, L. E., and Giusti, M. M. 2007. Mid-infrared Spectroscopy for Juice Authentication-rapid Differentiation of Commercial Juices. *Journal of Agricultural and Food Chemistry*. 55(11): 4443-4452.

[30] Lu, X., Wang, J., Al-Qadiri, H. M., Ross, C.F., Powers, J. R., Tang, J., and Rasco, B. A. 2011. Determination of Total Phenolic Content and Antioxidant Capacity of Onion (*Allium cepa*) and Shallot (*Allium oschaninii*) using Infrared Spectroscopy. *Food Chemistry*. 129(2): 637-644.

[31] Stuart, B.H. 2004. *Infrared Spectroscopy: Fundamentals and Applications*. England: John Wiley & Sons.

[32] Nakanishi, K., and Solomon, P. H. 1977. *Infrared Absorption Spectroscopy*. San Franciso: USA.

[33] Chis, A., Fetea, F., Taoutaou, A., and Socaciu, C. 2010. Application of FTIR Spectroscopy for a Rapid Determination of some Hydrolytic Enzymes Activity on Sea Buckthorn Substrate. *Romanian Biotechnological Letters*. 15(6): 5738-5744.

[34] Komoda, Y., Nakamura, H., Ishihara, S., Uchida, M., Kohda, H., and Yamasaki, K. 1985. Structures of New Terpenoid Constituents of *Ganoderma lucidum* (Fr.) Karst. (Polyporaceae). *Chemical and Pharmaceutical Bulletin*. 33(11): 4829-35.

[35] Agatonovic-Kustrin, S., Morton, D.W., and Yusof, A.P. 2013. The Use of Fourier Transform Infrared (FTIR) Spectroscopy and Artificial Neural Networks (ANNs) to Assess Wine Quality. *Modern Chemistry and Application*. 1(4): 1-8.
DOI:10.4172/2329-6798.1000110.

[36] Wang, Y., Xu, C.H., Wang, P., Sun, S.Q., Chen, J.B., Li, J., Chen, T., and Wang, J.B. 2011. Analysis and Identification of Different Animal Horns by a Three-stage Infrared Spectroscopy. *Spectrochimica Acta A*. 83(1): 265-270.

[37] Xu, C., Jia, X., Xu, R., Wang, Y., Zhou, Q., and Sun, S. 2013. Rapid Discrimination of Herba Cistanches by Multi-step Infrared Macro-fingerprinting Combined with Soft Independent Modeling of Class Analogy (SIMCA). *Spectrochimica Acta Part A: Molecular and Biomolecular Spectroscopy*. 114: 421-431.
DOI: http://dx.doi.org/10.1016/j.saa.2013.05.024.

[38] Choong, Y.K. 2017. *Fourier Transform Infrared and Two-Dimensional Correlation Spectroscopy for Substance Analysis*. In: Nicolic, G. *Fourier Transform*. 175-190. London: IntechOpen.

[39] Ozacar, M., Soykan, C., and Sengil, I.A. 2006. Studies on Synthesis, Characterization and Metal Adsorption of Mimosa and Valonia Tannin Resins. *Journal of Applied Polymer Science*. 102(1): 786-797.
DOI: https://doi.org/10.1002/app.23944.

[40] Su, X., Zhang, H., Shao, J., and Wu, H. W. 2007. Theoretical Study on the Structure and Properties of Crenulatin Molecule in Herb *Rhodiola crenulata*. *Journal of Molecular Structure*. 847(1-3): 59-67.
DOI: https://doi.org/10.1016/j.theochem.2007.08.034.

[41] Chis, A., Fetea, F., Matei, H., and & Socaciu, C. 2011. Evaluation of Hydrolytic Activity of Different Pectinases on Sugar Beet (*Beta vulgaris*) Substrate using FT-MIR Spectroscopy. *Notulae Botanicae Horti Agrobotanici Cluj-Napoca*. 39(2): 99-104.